Journal of The Electrochemical Society, **154** (3) H214-H216 (2007)
0013-4651/2007/154(3)/H214/3/$20.00 © The Electrochemical Society

Very High Density (44 fF/μm^2) $SrTiO_3$ MIM Capacitors for RF Applications

K. C. Chiang,[a,z] J. W. Lin,[b] H. C. Pan,[c] C. N. Hsiao,[c] W. J. Chen,[d] H. L. Kao,[e] I. J. Hsieh,[b] and Albert Chin[a,*]

[a]*Department of Electrical Engineering, Nano-Science Technology Center, National Chiao-Tung University, University System of Taiwan, Hsinchu, Taiwan*
[b]*Department of Electric Engineering, Chung Hua University, Hsinchu, Taiwan*
[c]*Instrument Technology Research Center, National Applied Research Laboratories, Hsinchu, Taiwan*
[d]*Graduate Institute of Materials Engineering, National Ping-Tung University of Science and Technology, Taiwan*
[e]*Department of Electronic Engineering, Chang-Gung University, Hsinchu, Taiwan*

We demonstrate a high-performance TaN/$SrTiO_3$/TaN metal-insulator-metal (MIM) radio-frequency (rf) capacitor with good device integrity of very high capacitance density of 44 fF/μm^2, small voltage linearity α of 54 ppm/V^2 at 2 GHz, and a small capacitance reduction 3.5% from 100 KHz to 10 GHz. Such large capacitance density can largely reduce the device size used in rf integrated circuits.
 [DOI: 10.1149/1.2431323]

Manuscript submitted May 10, 2006; revised manuscript received November 13, 2006. Available electronically January 19, 2007.

Based on the *International Technology Roadmap for Semiconductors (ITRS)*, continuous down-scaling of the device size of radio-frequency (rf) capacitors is needed to reduce the die size and lower the costs. To meet this requirement, higher capacitance density ($\varepsilon_0\kappa/t_d$) is required and using higher dielectric constant (κ) material is the only choice.[1-16] This is because the decreasing dielectric thickness (t_d) results in the degraded device performance of higher leakage current and poorer voltage-dependence of capacitance ($\Delta C/C$). Because the high κ strontium titanate ($SrTiO_3$)[17-19] dielectric has a very high κ value (reachable to 300) beyond HfO_2 (κ ~ 22 – 24), Nb_2O_5 (κ ~ 40),[11] TaTiO (κ ~ 45),[15,16] or HfTiO, it is important to study the possibility for rf applications. In addition, the $SrTiO_3$ (STO) is also listed in the DRAM manufacture roadmap,[20] and therefore the STO capacitor may be used for analog, rf, and dynamic random access memory (DRAM) simultaneously to realize low process costs and multifunctional system-on-chip (SoC). In this paper, we have studied STO metal-insulator-metal (MIM) capacitor for rf applications. Very high capacitance density of 44 fF/μm^2, high κ value of 147, and small $\Delta C/C$ of 752 ppm at 2 GHz were obtained at the same time, demonstrating the excellent device performance for rf applications.

Experimental

After depositing 2 μm of SiO_2 on Si wafer, the lower capacitor electrode was formed using plasma vapor deposited (PVD) TaN/Ta bi-layers. After patterning the bottom electrode, the TaN was treated by NH_3 plasma nitridation. Largely improved interfacial TaON formation, oxygen deficiency, and capacitance density degradation were achieved after post-deposition anneal (PDA).[21] Then, the 26 and 30 nm thick STO layers were deposited on the TaN/Ta electrode by PVD, followed by 450°C PDA for 1 h under oxygen environment. Finally, the TaN/Al was deposited and patterned to form the top capacitor electrode. The fabricated rf MIM capacitors were characterized using an HP4284A precision LCR meter to 1 MHz, and an HP8510C network analyzer for the S-parameter measurements to 10 GHz.[8,9] The series parasitic impedance and parallel rf pads were de-embedded from 'through' and 'open' transmission lines,[15,22] respectively. The capacitance at rf frequency was extracted from the measured S-parameters using an equivalent circuit model.[8,9,15,16]

Results and Discussion

Figures 1a and b show the capacitance-voltage (C-V) and current-voltage (*J-V*) characteristics of STO MIM capacitors, re-

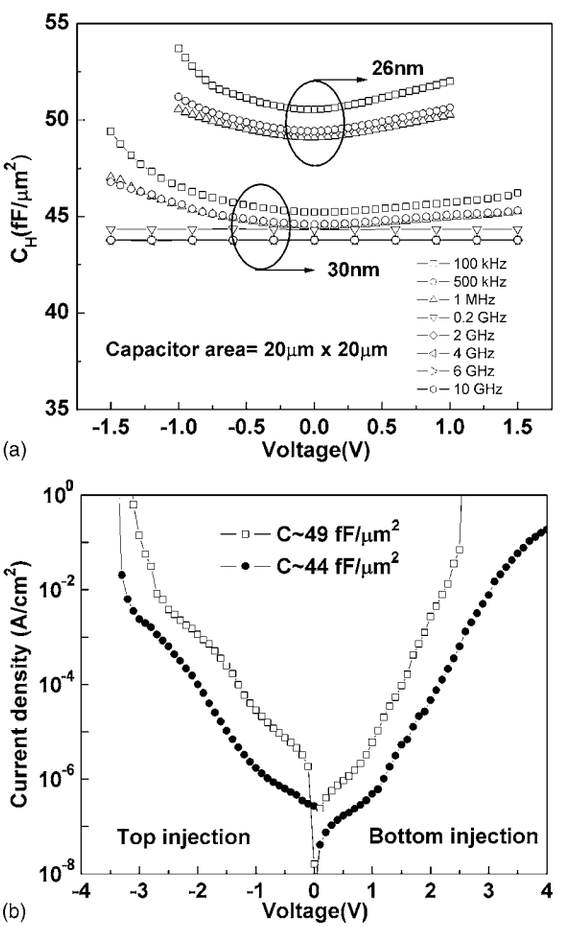

Figure 1. (a) C-V and (b) *J-V* characteristics of STO MIM capacitors. The C-V results from 100 kHz to 1 MHz are measured from LCR meter and the data from 0.2 GHz to 10 GHz was obtained from the S-parameters. High capacitance density of 44 and 49 fF/μm^2 were measured with low leakage density of 5 × 10^{-7} and 6 × 10^{-6} A/cm^2.

* Electrochemical Society Active Member.
z E-mail: gorden.ee91g@nctu.edu.tw

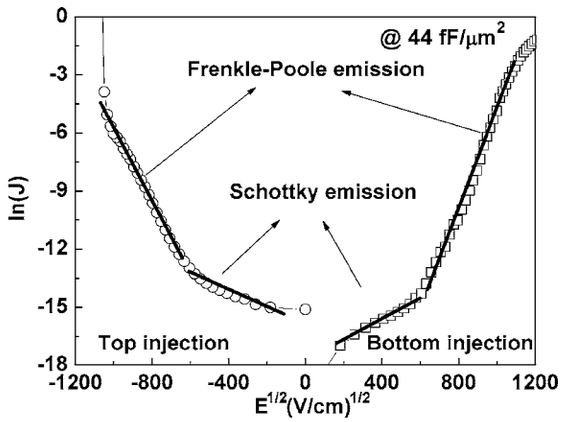

Figure 2. Measured and simulated J-$E^{1/2}$ of STO MIM capacitors.

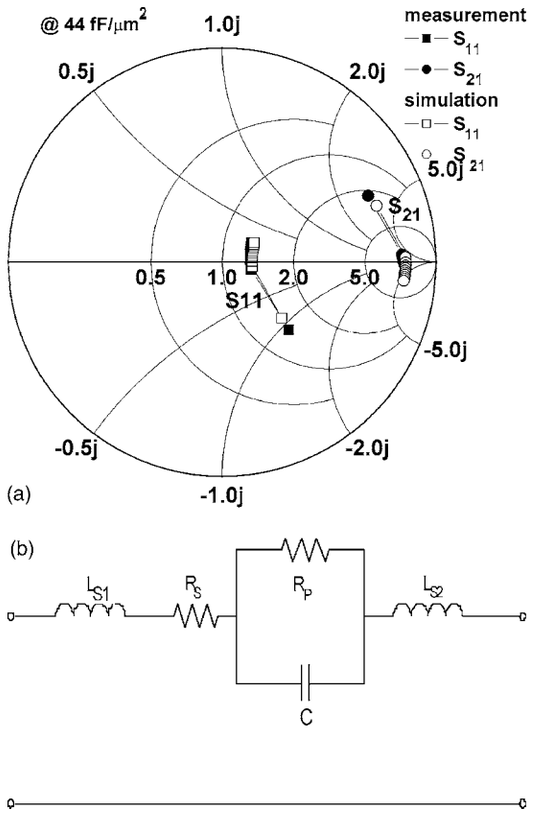

Figure 3. (a) Measured and simulated two-port S-parameters for STO MIM capacitors, from 500 MHZ to 10 GHz and (b) equivalent circuit model for capacitor simulation in rf regime.

spectively. Very high capacitance density of 44 and 49 fF/μm^2 or capacitance-equivalent thickness (CET) of 0.78 and 0.70 nm were measured with low leakage of 5×10^{-7} and 6×10^{-6} A/cm^2, respectively. Such small CET is useful for ITRS 45 nm node DRAM at year 2010. The leakage current under positive bias (electron injected from bottom TaN) is slightly lower than that under reverse bias (electron injected from top TaN). This may be due to the rough top STO surface from STO crystallization, which creates localized higher electric field in top TaN/STO. The surface roughness between dielectric and electrode is usually responsible for asymmetric performance of MIM capacitors.[23] In addition, note that the leakage current of 5×10^{-7} A/cm^2 is low enough for rf integrated circuit (IC) applications due to the very high capacitance density of 44 fF/μm^2: for a typically large 1 pF capacitor used in rf IC, the leakage current is as low as 0.1 pA at 1 V and significantly lower than the leakage current of sub-100 nm transistors.[22] Furthermore, a near constant capacitance value with little voltage and frequency dependence is obtained for the STO MIM capacitor, which is important for rf IC under large voltage swing condition.

To study the current conduction mechanism of TaN/STO/TaN MIM capacitors, we have plotted ln(J) vs $E^{1/2}$ in Fig. 2. Here, both Schottky emission (SE) and Frenkel-Poole (FP) conduction can give a linear ln(J)-$E^{1/2}$ relation with different slopes (γ), as shown by

$$J \propto \exp\left(\frac{\gamma E^{1/2} - V_b}{kT}\right) \quad [1]$$

$$\gamma = \left(\frac{e^3}{\eta\pi\varepsilon_0 K_\infty}\right)^{1/2} \quad [2]$$

where K_∞ is the high-frequency dielectric constant ($=n^2$; n is the refractive index and equals to 2.4 for STO[18,19]), and η is a constant with value of 1 or 4 for FP or SE, respectively. From the good matching between measured and Eq. 1 calculated data, the current conduction mechanism changes from SE at low electric fields to FP at higher fields.

To investigate the device rf characteristics of STO MIM capacitors, the S-parameters were measured. Figure 3a shows the measured S-parameters for TaN/STO/TaN capacitors, and the capacitance value is extracted by using the equivalent circuit model shown in Fig. 3b. The MIM capacitor is modeled by R_p and C, where the R_p originates from the high-κ dielectric loss. In addition, the R_s, L_{s1}, and L_{s2} represent the parasitic impedances in the coplanar transmission line used for rf measurements. Good matching between measured and modeled S-parameters are shown in Fig. 3a, indicating the good accuracy for capacitance extraction at rf regime beyond the limited 1 MHz of LCR meter.

The obtained capacitance density is plotted in Fig. 4a. Small capacitance reduction of only 3.5% to 10 GHz is indicative of the good device performance over the whole intermediate frequency (IF) to rf range.[6,7] However, such extracted capacitance density at the rf regime is not sensitive enough to calculate the small $\Delta C/C$ variation, important for precision capacitors operated under large signal swing. We have used the previous circuit-theory-derived equation[8] to calculate the $\Delta C/C$-V from measured S-parameters and the results are shown in Fig. 4b. The measured $\Delta C/C$-V can be fitted with a second order polynomial equation, where linear (β) and quadratic (α) voltage coefficients of $\Delta C/C$ were obtained. Because the β effect can be canceled by circuit design using differential method, α is the key parameter to cause the unwanted voltage-dependent $\Delta C/C$. The obtained $\Delta C/C$ and α are also plotted in Fig. 4a. Fortunately, both α and $\Delta C/C$ decrease with increasing frequency into the rf region, which is attributed to the trapped carriers being unable to follow the high-frequency signal with typical carrier lifetimes in the range ms to μs.[8,9,15,16] Therefore, high capacitance density of 44 fF/μm^2, small $\Delta C/C$ of 752 ppm, and low α of 54 ppm/V^2 at 2 GHz are important for high-speed rf IC applications.

The device quality (Q) factor and corresponding capacitance extracted from the circuit model[6] using the S-parameters at rf frequencies is shown in Fig. 5a. Note that a good Q-factor >50 is obtained for rf application before resonant frequency (f_r) of ~13 GHz, where the relative low f_r is due to the large capacitance. Furthermore, because the advanced ICs are usually operated at higher temperature due to power dissipation, the temperature-coefficient on capacitance (TCC) is another important factor. Figure 5b shows the TCC obtained from normalized capacitance of STO capacitor as a function of temperatures. Again, the TCC decreases with increasing frequency with TCC values close to previous TiTaO devices.[15]

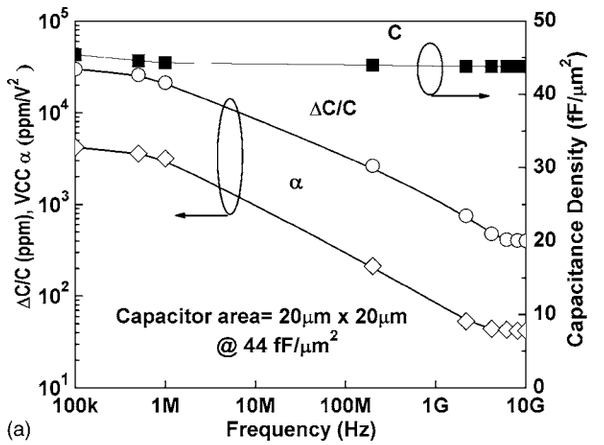

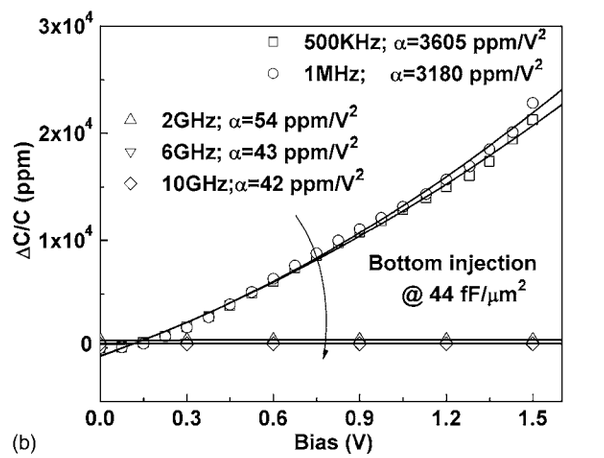

Figure 4. (a) Frequency dependent capacitance density, $\Delta C/C$, and α for a STO MIM capacitor biased at 1.5 V. The data for frequencies >1 MHz was obtained from the S-parameters. (b) The $\Delta C/C$-V characteristics of a STO MIM capacitor at rf regime.

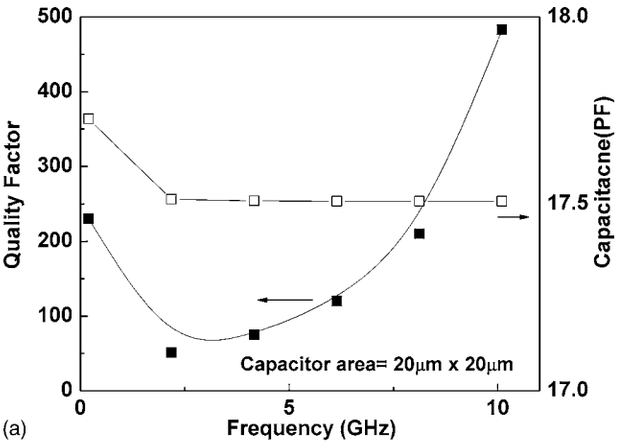

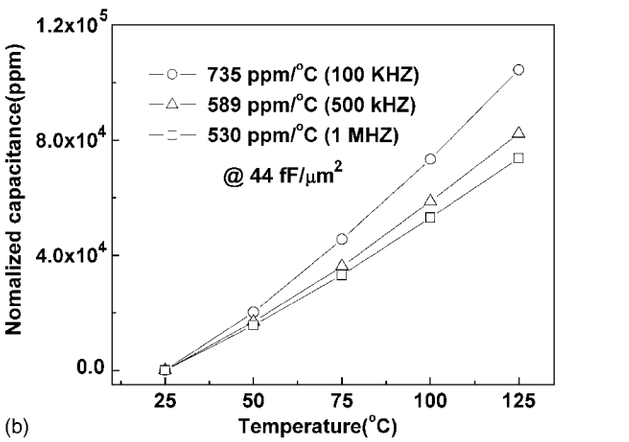

Figure 5. (a) *Q*-factor of TaN/STO/TaN MIM capacitors biased at 1.5 V (b) The temperature-dependent normalized capacitance (TCC) with different frequency. The capacitor size is 20 × 20 μm.

Conclusions

Very high 44 fF/μm^2 capacitance density, small capacitance reduction of 3.5% to 10 GHz, and a small α of 54 ppm/V^2 at 2 GHz were simultaneously achieved in TaN/STO/TaN capacitors processed at 450°C and important for rf application. This high-density MIM capacitor is important for down-scaling the capacitance size and integration with DRAM.

Acknowledgment

This work has been partially supported by NSC (95-2221-E-009-298) of Taiwan.

National Chiao Tung University assisted in meeting the publication costs of this article.

References

1. C. H. Ng, K. W. Chew, and S. F. Chu, *IEEE Electron Device Lett.*, **24**, 506 (2003).
2. L. Y. Tu, H. L. Lin, L. L. Chao, D. Wu, C. S. Tsai, C. Wang, C. F. Huang, C. H. Lin, and J. Sun, in *Proceedings of the Symposium on VLSI Technology*, IEEE, p. 79 (2003).
3. Z. Chen, L. Guo, M. Yu, and Y. Zhang, *IEEE Microw. Wirel. Compon. Lett.*, **12**, 246 (2002).
4. J. A. Babcock, S. G. Balster, A. Pinto, C. Dirnecker, P. Steinmann, R. Jumpertz, and B. El-Kareh, *IEEE Electron Device Lett.*, **22**, 230 (2001).
5. C.-M. Hung, Y.-C. Ho, I.-C. Wu, and K. O, *IEEE Trans. Microwave Theory Tech.*, **46**, 505 (1998).
6. S. B. Chen, J. H. Lai, K. T. Chan, A. Chin, J. C. Hsieh, and J. Liu, *IEEE Electron Device Lett.*, **23**, 203 (2002).
7. S. B. Chen, J. H. Lai, A. Chin, J. C. Hsieh, and J. Liu, *IEEE Electron Device Lett.*, **23**, 185 (2002).
8. C. H. Huang, M. Y. Yang, A. Chin, C. X. Zhu, M. F. Li, and D. L. Kwong, in *Proceedings of the IEEE MTT-S International Microwave Symposium*, IEEE, p. 507 (2003).
9. M. Y. Yang, C. H. Huang, A. Chin, C. Zhu, B. J. Cho, M. F. Li, and D. L. Kwong, *IEEE Microw. Wirel. Compon. Lett.*, **13**, 431 (2003).
10. C. Zhu, H. Hu, X. Yu, A. Chin, M. F. Li, and D. L. Kwong, *Tech. Dig. - Int. Electron Devices Meet.*, **2003**, 379.
11. S. J. Kim, B. J. Cho, M.-F. Li, C. Zhu, A. Chin, and D. L. Kwong, in *Proceedings of the Symposium on VLSI Technology*, IEEE, p. 77 (2003).
12. S. J. Kim, B. J. Cho, M.-F. Li, S.-J. Ding, C. Zhu, M. B. Yu, B. Narayanan, A. Chin, and D.-L. Kwong, *IEEE Electron Device Lett.*, **25**, 538 (2004).
13. S. J. Kim, B. J. Cho, M. B. Yu, M.-F. Li, Y.-Z. Xiong, C. Zhu, A. Chin, and D. L. Kwong, in *Proceedings of the Symposium on VLSI Technology*, IEEE, p. 56 (2005).
14. S. J. Kim, B. J. Cho, M. B. Yu, M. F. Li, Y. Z. Xiong, C. Zhu, A. Chin, and D. L. Kwong, *IEEE Electron Device Lett.*, **26**, 625 (2005).
15. K. C. Chiang, C. H. Lai, A. Chin, T. J. Wang, H. F. Chiu, J. R. Chen, S. P. McAlister, and C. C. Chi, *IEEE Electron Device Lett.*, **26**, 728 (2005).
16. K. C. Chiang, A. Chin, C. H. Lai, W. J. Chen, C. F. Cheng, B. F. Hung, and C. C. Liao, in *Proceedings of the Symposium on VLSI Technology*, IEEE, p. 62 (2005).
17. P.-Y. Lesaicherre, S. Yamamichi, H. Yamaguchi, K. Takemura, H. Watanabe, K. Tokashiki, K. Satoh, T. Sakuma, M. Yoshida, S. Ohnishi, K. Nakajima, K. Shibahara, Y. Miyasaka, and H. Ono, *Tech. Dig. - Int. Electron Devices Meet.*, **1994**, 831.
18. C.-J. Peng, H. Hu, and S. B. Krupanidhi, *Appl. Phys. Lett.*, **63**, 1038 (1993).
19. F. Gervais, in *Handbook of Optical Constants of Solids*, E. D. Palik, Editor, p. 1035, Academic Press, New York (1991).
20. K. Kim, *Tech. Dig. - Int. Electron Devices Meet.*, **2005**, 333.
21. K. C. Chiang, C. C. Huang, A. Chin, G. L. Chen, W. J. Chen, Y. H. Wu, and S. P. McAlister, *IEEE Trans. Electron Devices*, **53**, 2312 (2006).
22. M. C. King, Z. M. Lai, C. H. Huang, C. F. Lee, D. S. Yu, C. M. Huang, Y. Chang, and Albert Chin, in *Proceedings of the IEEE RF-IC Symposium*, IEEE, p. 171 (2004).
23. N. Gaillard, L. Pinzelli, and G.-J. Mickael, *Appl. Phys. Lett.*, **89**, 133506 (2006).